



HAL
open science

Quantitative variations of the mitochondrial proteome and phosphoproteome during fermentative and respiratory growth in *Saccharomyces cerevisiae*

Margaux Renvoisé, Ludovic Bonhomme, Marlène Davanture, Benoît Valot, Michel Zivy, Claire Lemaire

► To cite this version:

Margaux Renvoisé, Ludovic Bonhomme, Marlène Davanture, Benoît Valot, Michel Zivy, et al.. Quantitative variations of the mitochondrial proteome and phosphoproteome during fermentative and respiratory growth in *Saccharomyces cerevisiae*. *Journal of Proteomics*, 2014, 106, pp.140-150. 10.1016/j.jprot.2014.04.022 . cea-02462405

HAL Id: cea-02462405

<https://cea.hal.science/cea-02462405>

Submitted on 31 Jan 2020

HAL is a multi-disciplinary open access archive for the deposit and dissemination of scientific research documents, whether they are published or not. The documents may come from teaching and research institutions in France or abroad, or from public or private research centers.

L'archive ouverte pluridisciplinaire **HAL**, est destinée au dépôt et à la diffusion de documents scientifiques de niveau recherche, publiés ou non, émanant des établissements d'enseignement et de recherche français ou étrangers, des laboratoires publics ou privés.

Quantitative variations of the mitochondrial proteome and phosphoproteome during fermentative and respiratory growth in *Saccharomyces cerevisiae*

Margaux Renvoisé a,b ; Ludovic Bonhomme c ; Marlène Davanture d ; Benoit Valot c ; Michel Zivy d ; Claire Lemaire a, b

- a) CNRS, UMR8221, F-91191 Gif-sur-Yvette, France
- b) CEA, IBITECS, SB2SM, LPM, F-91191 Gif-sur-Yvette, France
- c) INRA, PAPPSO, UMR de Génétique Végétale, Gif-sur-Yvette, France
- d) CNRS, PAPPSO, UMR de Génétique Végétale, Gif-sur-Yvette, France

Abstract

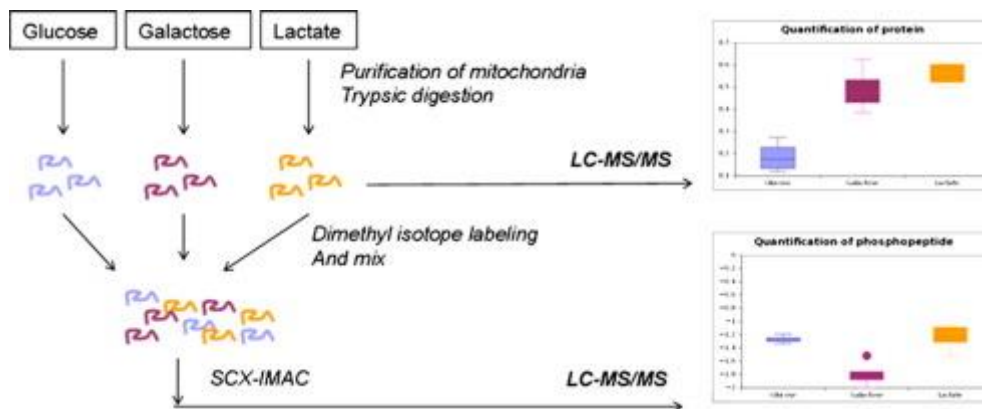
The yeast *Saccharomyces cerevisiae* is a facultative aerobe able to adapt its metabolism according to the carbon substrate. The mechanisms of these adaptations involve at least partly the mitochondria but are not yet well understood. To address the possible role of protein phosphorylation event in their regulation, it is necessary in a first instance to determine precisely the phosphorylation sites that show changes depending on the carbon source. In this aim we performed an overall quantitative proteomic and phosphoproteomic study of isolated mitochondria extracted from yeast grown on fermentative (glucose or galactose) and respiratory (lactate) media. Label free quantitative analysis of protein accumulation revealed significant variation of 176 mitochondrial proteins including 108 proteins less accumulated in glucose medium than in lactate and galactose media. We also showed that the responses to galactose and glucose are not similar. Stable isotope dimethyl labeling allowed the quantitative comparison of phosphorylation levels between the different growth conditions. This study enlarges significantly the map of yeast mitochondrial phosphosites as 670 phosphorylation sites were identified, of which 214 were new and quantified. Above all, we showed that 90 phosphosites displayed a significant variation according to the medium and that variation of phosphorylation level is site-dependent.

Biological significance

This proteomic and phosphoproteomic study is the first extensive study providing quantitative data on phosphosites responses to different carbon substrates independent of the variations of protein quantities in the yeast *S. cerevisiae* mitochondria. The significant changes observed in the level of

phosphorylation according to the carbon substrate open the way to the study of the regulation of mitochondrial proteins by phosphorylation in fermentative and respiratory media. In addition, the identification of a large number of new phosphorylation sites show that the characterization of mitochondrial phosphoproteome is not yet completed.

Graphical Abstract



1. Introduction

Mitochondrion is an organelle with multiple functions, the most important of which being to provide energy to the rest of the cell in the form of ATP by oxidative phosphorylation, a process catalyzed by the respiratory enzymes organized in supercomplexes in the mitochondrial inner membrane [1,2]. In humans, deregulation of mitochondrial functions, in particular of the respiratory chain, is associated with several pathologies, including neurodegenerative diseases [3,4], neuromuscular diseases [5], type II diabetes [6] and cancer [7]. In response to metabolic demand or various stresses, the activity of the respiratory enzymes may be adjusted and several levels of regulation could be conceived such as change in the expression level of proteins, reversible interaction with effectors, or post-translational modifications such as phosphorylation. In plants, phosphorylation was shown to play a regulatory role in response to light conditions by inducing change in the supramolecular organization and the activity of photosynthetic apparatus of the chloroplast, an energy-converting organelle that is related to the mitochondrion [8]. The steadily increasing number of known mitochondrial phosphoproteins, kinases and phosphatases suggests that reversible protein phosphorylation could be an important level of regulation in mitochondria [9] and could be partly responsible for an adaptation to environmental change as it is the case for chloroplasts [10]. Testing such hypothesis cannot be considered without quantitative data on the variations of mitochondrial protein amounts and their level of phosphorylation under several growth conditions. The yeast

Saccharomyces cerevisiae is a powerful tool to study various energetic and physiological states as it is a facultative aerobe which can grow either on fermentative substrate such as glucose or galactose or on respiratory substrate such as lactate. Few global quantitative phosphoproteomic and proteomic studies have been carried on yeast grown on different carbon sources but mostly on whole cell extracts [11,12] and the lack of subfractionation limited the access of information on mitochondrial proteins. Two qualitative studies focused on a subset of mitochondrial proteins, but the use of 2D gel electrophoresis [13,14] limited the access to hydrophobic or basic proteins and to those of very high or very low molecular weight. In this paper, we present for the first time a quantitative study of both protein abundance and phosphorylation levels in isolated yeast mitochondria, under respiratory (lactate medium) or fermentative conditions with two different substrates (glucose and galactose). We performed a subcellular fractionation to focus our analysis specifically on the mitochondrial proteins and used LC-MS/MS to overcome the limitations of 2D gel electrophoresis [15–17]. Protein abundances were quantified using a label free method. The quantitative analysis of the phosphoproteome was carried out by using the multiplex stable isotope dimethyl labeling procedure [18]. For all quantified phosphopeptides, protein abundance measurements were performed allowing normalization of the data and providing a way to analyze the specific variation of phosphorylation status independent of the protein abundance changes. Finally, this study allowed us to obtain a reliable description of the adaptation of the yeast mitochondrial proteome and phosphoproteome to different carbon sources.

2. Material and methods

2.1. Cell culture of yeast

The yeast wild strain W303 (aade2-1 ura3-1 his3-11,15 trp1-1 leu2-3,112 can1-100) was grown either in 2% glucose medium (YPGA) to an $OD_{600} = 6$, or 2% galactose medium (YPGAL) to an $OD_{600} = 6$ or 2% lactate medium (YLAC) to an $OD_{600} = 4.5$ media as described in Lemaire and Dujardin [19]. Four independent biological replicates were performed in each growth condition, leading to 12 samples in total.

2.2. Extraction of mitochondria

Extraction of mitochondria was performed using the protocol originally developed by Meisinger et al. [20] and widely used in proteomic studies in yeast (see Reinders et al., [21]). Briefly, crude mitochondrial fraction was

prepared by differential centrifugation and adjusted to a protein concentration of 5 mg/mL in 250 mM sucrose/1 mM EDTA/10 mM Mops, pH 7.2. After treatment with 10 pestle strokes in a glass-Teflon potter, mitochondria were loaded on top of a three-step sucrose gradient. The proteins were then precipitated by 10% TCA, washed by acetone and stored at -20°C .

2.3. In solution digestion.

Precipitated proteins from each sample were suspended in buffer A (0.1% ZALSI, 6 M urea, 2 M thiourea, 10 mM DTT, 30 mM Tris-HCl pH 8.8, 5 mM NH_4HCO_3). Protein concentration was measured using the 2-D Quant Kit (GE Healthcare, Piscataway, NJ, USA) with BSA as a standard. For each sample, 1.3 mg of protein was incubated in the dark for 1 h with iodoacetamide to a final concentration of 40 mM and then diluted 8-fold with 50 mM NH_4HCO_3 . Samples were digested in-solution overnight at 37°C by adding 40 μg of trypsin in 200 μL of 50 mM NH_4HCO_3 (trypsin/protein ratio: 1/32.5). Trypsin digestion was stopped by addition of TFA to pH 2. An aliquot of each sample was kept at -20°C for further study of the global proteome.

2.4. Stable isotope dimethyl labeling of tryptic peptides

Trypsin digest of each sample was dried by vacuum centrifugation and re-suspended in 1 mL of 5% formic acid. Trypsin peptides were labeled on column by multiplex stable isotope dimethyl labeling procedure as described in Boersema [18]. Briefly the peptides are labeled on their primary amines which are converted to dimethylamines. Several isotopomers of formaldehyde and cyanoborohydride were used to add a specific mass (28, 32 or 36 Da) to the labeled peptide. Each SepPak C18 cartridge column (3 cc; Waters) was conditioned with 2 mL of acetonitrile (ACN) and equilibrated with 2×2 mL of buffer B (0.6% acetic acid in bi-distilled water). Each sample was loaded in a separate column and washed with 2 mL of buffer B. Each column was flushed 7 times by 1 mL of a labeling solution. The columns were then washed with 2 mL of buffer B. Peptides were eluted with 2×500 μL of buffer C (0.6% acetic acid in 80% ACN). Light, intermediate and heavy labeled peptides were mixed in a 1:1:1 ratio. One mix per biological replicate was prepared. Each mix contained samples from the three growth conditions, and each growth condition was alternatively labeled with a light, intermediate and heavy isotope in the four replicates. Light label corresponds to lactate medium in replicates 1 and 2, to glucose medium in replicate 3 and to galactose medium in replicate 4. Intermediate label corresponds to galactose medium in

replicates 1 and 2, to lactate medium in replicate 3 and to glucose medium in replicate 4. Heavy label corresponds to glucose medium in replicates 1 and 2, to galactose medium in replicate 3 and to lactate medium in replicate 4.

2.5. Sample fractionation by strong cation exchange chromatography

Labeled peptides were dried by vacuum centrifugation and re-suspended in 500 μ L of buffer D (ACN/H₂O: 30/70, 0.5% formic acid, pH 2). It was fractionated by Strong-Cation Exchange Chromatography according to Bonhomme et al.[22], using a Zorbax Bio SCX-Series II column (0.8 mm innerdiameter \times 50 mm length; 3.5 μ m particle size) on a Ulti-mate LC system combined with a Famos autosampler and a Switchos II microcolumn switch system (LC Packings, Sunnyvale, CA, USA). Chromatographic separation was made by a binary buffer system, constituted by buffer D and buffer E (buffer E: ACN/H₂O: 30/70, 0.5% formic acid, 50 mM Ammonium formate, pH 5) at a flow rate of 200 μ L/min for 80 min. Sample was automatically collected in a 96 well plate collector, using an on-line Probot system (LC Packings) to form 12 fractions.

2.6. Enrichment of phosphopeptides by Immobilized Metal ion Affinity Chromatography

Each fraction was dried by vacuum centrifugation and re-suspended in 300 μ L of loading buffer (H₂O/ACN: 70/30, with 250 mM acetic acid). For each fraction, 80 μ L of Phos-Select Iron Affinity Gel[22] was washed 4-fold with loading buffer and added to the fraction. Peptides were incubated with Phos-select Affinity Gel during 1 h, using a tube rotator. Phos-select Affinity Gel was washed in SigmaPrep spin column (Sigma Aldrich, St Louis, USA), twice with 200 μ L of loading buffer and once with 200 μ L of bidistilled water. Phosphopeptides were then eluted in SigmaPrep spin column with 2 \times 30 μ L of elution buffer (H₂O/ACN: 70/30, 0.4 M ammonium hydroxide). Eluted phosphopeptides were dried by vacuum centrifugation and kept at -20 °C until LC-MS/MS analysis. Twenty four percent of the identified peptides were phosphorylated in the enriched fractions. This result shows that the enrichment was very effective, since only 4 phosphopeptides can be detected in non-enriched samples. Interestingly, 88% of the unphosphorylated peptides contained at least one Asp or Glu, which confirms the known limit of the IMAC methodology with regards to the strong affinity for acidic peptides.

2.7. LC–MS/MS analysis

Each sample was resuspended in 20 μ L of 0.1% formic acid in 2% ACN (solvent E) then 4 μ L were loaded at 7.5 μ L/min on a pre-column cartridge (stationary phase: C18 PepMap 100, particles of 5 μ m; column: 100 μ m i.d., 1 cm length; Dionex) using a Nano LC-Ultra system (Eksigent, AB SciEX Massachusetts, USA). Peptides were desalted with solvent E during 3 min and loaded on a separating PepMap C18 column (stationary phase C18PepMap 100, particles of 3 μ m; column 75 μ m i.d., 150 mm length; Dionex) prior to gradient chromatography. The buffers used were 0.1% formic acid in water (solvent F) and 0.1% formic acid in ACN (solvent G). A 37 min-long linear gradient from 5 to 30% G at 300 nL/min was used for peptide separation. Including the regeneration step at 95% G and the equilibration step at 95% F; each run took 45 min. Eluted peptides were analyzed with a Q-Exactive mass spectrometer (Thermo Electron, Courtaboeuf, France) using a nano-electrospray interface. Ionization was performed with a 1.3-kV spray voltage applied to an uncoated capillary probe (10 μ i.d.; New Objective, Woburn, MA, USA). Xcalibur 2.1 interface was used to monitor data-dependent acquisition of peptide ions. This included a full MS scan covering the 300 to 1400 mass-to-charge ratio (m/z) with a resolution of 70,000 and a MS/MS step (normalized collision energy: 30%; resolution: 17,500). The MS/MS step was reiterated for the 8 major ions detected during the full MS scan. The dynamic exclusion was set to 45 s. For the analysis of total protein content, 1 μ g of digest from each of the 12 samples was directly submitted to LC–MS. The methods were the same as those described for phosphopeptides, except that the duration of the LC gradient separation was increased to 1 h.

2.8. Identification of peptides and phosphorylation sites

Database searches were performed using X!Tandem CYCLONE (<http://www.thegpm.org/TANDEM>). Cys carboxyamidomethylation and light, intermediary and heavy dimethylation of peptide N-termini and lysine residues were set as static modifications while methionine oxidation and phosphorylation of tyrosine were set as variable modifications. Serine and threonine residues phosphorylation was searched as variable modification motifs including phosphate loss. Precursor mass tolerance was 10 ppm and fragment mass tolerance was 0.02 Th. Identifications were performed using the Saccharomyces Genome Database, (<http://www.yeastgenome.org/>, release number: R63-1-1, release date: 20100105, S288C_reference_genome_R63-1-1_20100105) to which common contaminants were added. Identified proteins were filtered and grouped using the X!Tandem pipeline v3.3.0 (<http://pappso.inra.fr/bioinfo/xtandempipeline/>). Data filtering was

achieved according to a peptide E value smaller 0.01. Using such a threshold, the false discovery rate (FDR) was estimated to 0.5%.

2.9. Relative quantification of peptides and proteins

Mass ChroQ [23] was used for the alignment of LC–MS runs and peptide quantification by integration of extracted ion current (10 ppm window) in the peak detected at the expected retention time. Normalization was performed to take into account possible global variations between samples: for each LC–MS run the ratio of all peptide values to their value in a chosen reference LC–MS run was computed, and normalization was performed by dividing peptide values by the median value of peptide ratios. Only peptides which have been quantified in at least 3 replicates per condition were kept for protein quantification. Only proteins quantified with at least two peptides were kept. Statistical tests were performed on log₁₀-transformed data. The effect of growth condition on each protein was tested by using its normalized peptide values in a mixed model of analysis of variance, with growth conditions as a fixed effect and the peptides and the sample as random effects. We used the `fdrtool` library of the R package to compute the classical False Discovery Rate [24]. The effect of the growth condition was considered significant when the q-value (False Discovery Rate adjusted p-value) was <0.01.

2.10. Relative quantification of phosphopeptides and statistical analyses

As for the analysis of protein abundance, the quantification of phosphopeptides was performed using MassChroQ [23]. The alignment was performed between LC–MS/MS runs originating from the same SCX fraction of the different replicates. In the following, a replicate designates the mix of 3 samples corresponding to 3 different growth conditions, each sample being labeled with a different isotope, and a triplex designates the set of isotopes for a same m/z in the same fraction. As there were 12 SCX fractions, each replicate was represented by 12 LC–MS runs. For a given peptide, a triplex in a fraction was quantified only when at least 2 isotopes were detected. For normalization, we used a method similar to the one used for protein quantification, i.e. based on the principle that the median ratio between isotopic peptides within a replicate (i.e. within a mix of 3 samples labeled with different isotopes) must be equal to 1 [22]. After log₁₀-transformation of normalized data, phosphopeptide variations according to the growth condition were determined by using a mixed model of analysis of variance with the treatment (i.e. the corresponding isotope) as a fixed effect and with the triplex and replicate

as random effects. Finally, the relative level of phosphorylation of a protein was computed by dividing the phosphopeptide by the unphosphorylated protein content estimated by the two ANOVA models. As phosphopeptides and peptides used to measure protein abundance are different, the computed ratio does not represent a real estimation of the relative level of protein phosphorylation, but this normalization allowed making the phosphorylation value independent from protein amount variation. A simple ANOVA model was used to analyze changes, with only the growth condition as a fixed effect. It was considered significant when the FDR adjusted p-value was <0.05 . The analysis of qualitative variations was based on the detection of MS peaks. A K-means clustering was done on proteins whose abundance changed significantly according to growth conditions. Another was done on phosphorylation sites whose level varied according to growth conditions. For these 2 K-means analyses, the dissimilarity criterion was the Pearson correlation and the maximal iterations were 50.

3. Results and discussion

3.1. Variations of mitochondrial protein abundances during fermentative and respiratory growth

We quantified 724 proteins, of which 75% (544 proteins) were known to be mitochondrial proteins and only these were used for further data treatment (see Supplemental data S1). The other 25% proteins were essentially from the polysomes (11%) which are known to be bound to mitochondria [25]. The other contaminants were essentially of cytoplasmic (8%) or nuclear (2%) origin. Among these 724 proteins, the abundance of 368 displayed no change according to the growth medium while 176 proteins varied significantly. A classification was performed on this set of 176 proteins which defined 4 clusters (Fig. 1 and Supplemental data S2). For each cluster, the different abundance factors relating to the three growth media were compared pair wise (see Table 1). This approach allowed defining two major groups (see Fig. 1 and Table 1) showing that the most extreme differences are between glucose and lactate media. One group includes proteins more abundant in glucose than in lactate by a factor varying between 1.9 and 7.5 (cluster 1; 68 proteins i.e. 39%). The second group is defined by proteins more abundant in lactate than in glucose (clusters 2 to 4; 108 proteins i.e. 61%) with an average abundance factor varying from 0.26 to 0.42. Interestingly, we highlighted significant differences between the two fermentative substrates studied as, in most of the cases (clusters 1 to 3), protein abundance in galactose medium displays a different pattern than in glucose medium (average abundance factor varying from 0.55 to 2.9). In clusters 1 and 3, the galactose medium

was intermediary between the glucose and lactate media. In cluster 2, the same pattern is observed for galactose and lactate. Finally, cluster 4 is the only one which contained proteins whose abundance in galactose and glucose were almost similar. Few studies have already compared protein amounts between fermentation and respiration at the steady-state level [12,26,27]. Moreover these analyses were performed on whole cell extracts and only some few data on mitochondrial proteins were found. Our study allows for the first time a overall comparison of mitochondrial protein abundances in fermentation and respiration together with a deeper analysis of differences between two fermentative substrates which suggest that galactose could be finally considered as a substrate displaying an intermediate metabolism between fermentation (glucose medium) and respiration (lactate medium). This is supported by the data indicating that the contribution of respiration has been shown to be larger during growth on galactose than in glucose [28]

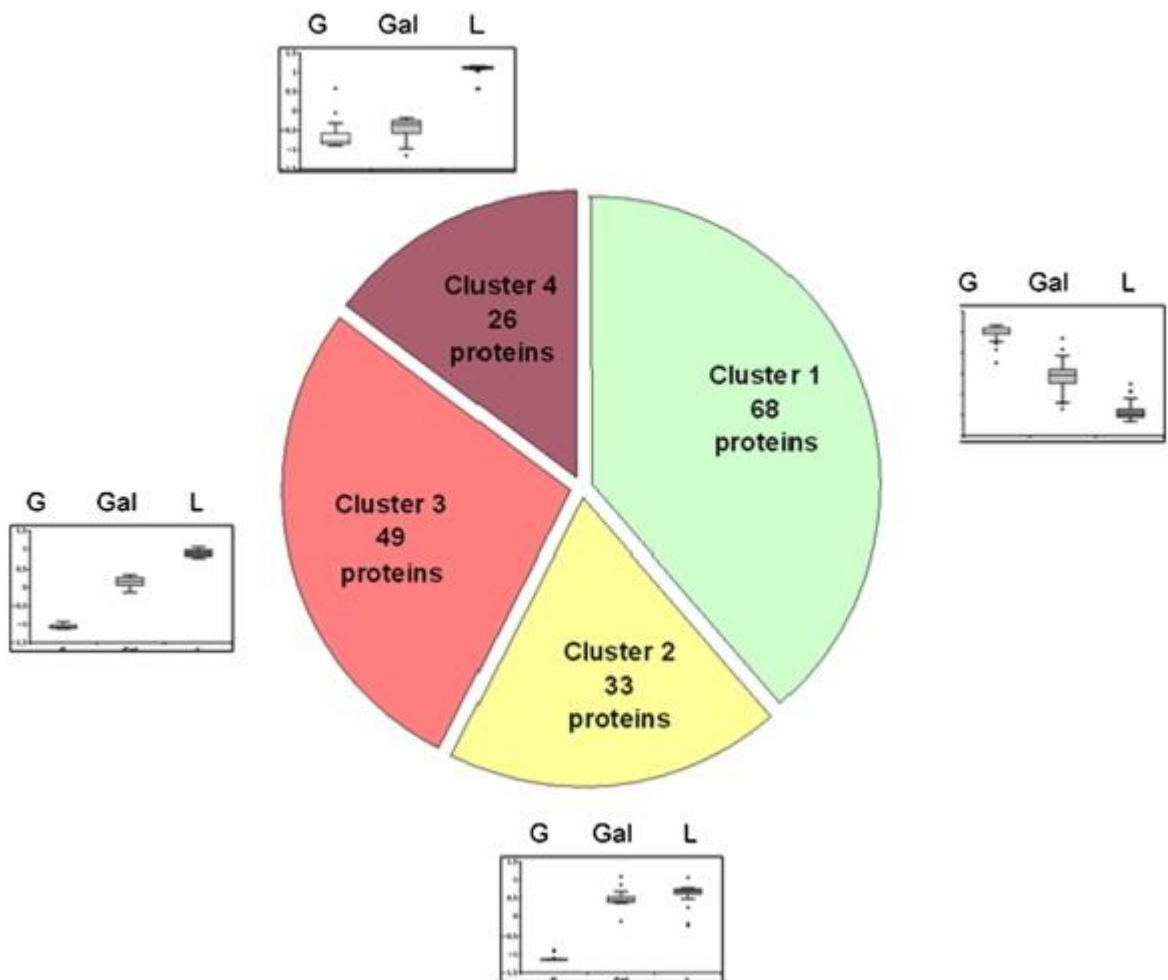


Fig. 1–Significant changes of protein abundances according to the substrate. Pie graph of the clusters built for proteins whose abundance was significantly

affected by the substrate (K-means clustering) (G = glucose; Gal = galactose; L = lactate). Box plots are depicted beside their respective shares. The number of proteins associated to each of the four defined clusters is given.

The protein composition of the clusters will be presented and discussed later in the section concerning the comparison between variation of mitochondrial protein abundances and protein phosphorylation according to their metabolic path-ways. To facilitate this comparison, the clusters were defined by their major trend. Cluster 1 was considered as lactate⁻ (LAC⁻), clusters 2 and 3 were gathered and defined as glucose⁻ (GLU⁻) and cluster 4 as lactate⁺ (LAC⁺).

3.2. Mitochondrial protein phosphorylation display qualitative and quantitative variations between fermentative and respiratory growth

Table 1–Variations of protein abundances according to the cluster. The mean and standard deviation of the ratio between the abundance in one condition and the abundance in the other are shown for every comparison between two substrates and for every cluster.

	Glucose/lactate	Galactose/lactate	Galactose/glucose
Cluster 1	4.7 ± 2.8	2.0 ± 0.58	0.55 ± 0.09
Cluster 2	0.42 ± 0.08	0.92 ± 0.11	2.5 ± 0.67
Cluster 3	0.26 ± 0.08	0.57 ± 0.09	2.9 ± 0.72
Cluster 4	0.28 ± 0.12	0.32 ± 0.11	1.4 ± 0.30

The mitochondrial phosphoproteome of yeast cultivated in three different sources of carbon was investigated using the multiplex stable isotope dimethyl labeling procedure for relative quantification which labeling efficiency was estimated between 93 and 97.7%. Our mitochondrial phosphoproteome analysis led to the identification of 670 phosphorylation sites, observed in at least one of the 12 samples (Supplemental data S3, S4 and S5). Ninety eight percent of the spectra that identified the same phosphopeptide were found in at most three SCX fractions and 50% were found in the same fraction. The phosphopeptides were identified in 299 proteins of which 150 displayed one site of phosphorylation, 72, two sites, 27, three sites and 50, four sites or more (http://moulon.inra.fr/protic/yeast_mitochondria, <http://www.proteomexchange.org> and Supplemental data S3). In total, 71% of them were serine, 16% were threonine and 0.6% were tyrosine. 12.4% of the residues could not be precisely localized in the peptide sequence.

We considered here only the 289 phosphosites which were present in at least 3 biological replicates in 1, 2 or 3 conditions (Supplemental data S6 and S7). Among them, 214 were not identified in previous studies [11,21,29] (Supplemental data S6). Thus our present work enlarges significantly the map of yeast mitochondrial phosphosites.

3.2.1. Variations in the three growth conditions

Among the 289 phosphosites reproducibly quantified in 1, 2 or 3 conditions, the majority (238 phosphosites) were reproducibly quantified in the three growth conditions and were subjected to quantitative examination using analysis of variance. To estimate as precisely as possible the variations of protein phosphorylation independent of protein amount variations, all phosphopeptide data were normalized according to protein abundance by dividing the phosphopeptide quantitative values by the protein abundance values. The mean coefficient of variation of the \log_{10} -transformed ratio was 1.86%.

39 phosphorylation sites significantly varied according to carbon substrate (Supplemental data S8) while 199 displayed no significant change under our experimental conditions (Supplemental data S9). A classification based on the normalized quantification of these 39 phosphorylation sites was performed (Fig. 2 and Supplemental data S10). We could isolate five clusters of phosphorylation sites. Clusters P1 to P4 displayed the same pattern as those observed for the clusters 1 to 4 defined for protein abundances. Indeed, the abundance factors of the phosphopeptides were of the same order of magnitude than those of protein abundances for a given cluster (see Table 2). An additional cluster P5 included three sites that were less phosphorylated in galactose than in glucose (a decrease by a factor 5) and lactate (a decrease by a factor 2.5). This suggests that a specific regulation could occur in galactose, independently from the two other conditions.

3.2.2. Variations in one or two growth conditions

In addition to the 238 sites reproducibly quantified in the three growth conditions, we also observed 51 sites showing a variation in 1 or 2 conditions as they were absent in the 4 biological replicates of the (se) condition(s) (see Table 3). In the following sections, we gathered phosphorylation sites displaying variations either in one or two growth conditions (51 residues, Table 3) or in the three simultaneously (39 residues, Supplemental data S5). As for the protein abundances, we grouped the sites according to their major trend. The 29 sites detected only in glucose and/or galactose and the 7 sites of cluster P1 were

considered as LAC⁻, the 16 sites detected only in lactate and galactose and 24 sites of clusters P2 + P3 as GLU⁻; the 2 sites only detected in lactate and glucose and the 3 sites of cluster P5 as GAL⁻ and finally the 4 only detected in lactate and the 5 sites of cluster P4 as LAC⁺.

Table 2–Variations of phosphopeptide abundances according to the cluster. The mean and standard deviation of the ratio between the abundance in one condition and the abundance in the other are shown for every comparison between two substrates and for every cluster.

	Glucose/lactate	Galactose/lactate	Galactose/glucose
Cluster P1	4.5 ± 1.5	2.1 ± 0.24	0.60 ± 0.15
Cluster P2	0.37 ± 0.08	1.1 ± 0.18	3.4 ± 0.67
Cluster P3	0.44 ± 0.50	0.45 ± 0.18	2.2 ± 0.44
Cluster P4	0.18 ± 0.04	0.21 ± 0.06	1.1 ± 0.11
Cluster P5	2.8 ± 1.1	0.42 ± 0.0	80.20 ± 0.05

Table 3

Growth condition	Gene	Metabolic pathway	Phosphorylation site	Phosphopeptide
Glucose (5)	CBP3	Mitochondria biogenesis	S44	ETAQDpSPPELLAK
	HER1	Unknown	S1192	VGLEpSLYGDDELNSR
	TIF4631	Protein synthesis	T177	LKETSdSpTSTSTPTPTSTNDK
	WWM1	Cell rescue, defense and virulence	S131	YYPQQAAMPAAAPQQAAYYGTApPpSTSK
	YSP2	Unknown	S399	NVNANSNpSETENDNDRDDR
Galactose + Glucose (24)	BAT1	Amino acid metabolism	S26	LATGAPLDApSKLK
	CYC7	Energy	S57	GYPsYTDANINK
	CYS4	Amino acid metabolism	S350	FDpSSKLEASTTK
	FCJ1	Mitochondria biogenesis	S113	SBDLLSGLTGpSSQTR
	GPB2	Cellular communication / signal transduction	S24	VAVpSPFFSALEGEER
	GPM1	C-compound and carbohydrate metabolism	S116	pSFDVPPPPIDASSPFSQK
	HER1	Unknown	S1013	ADNpSPFNIGDSTVSNANYNDGIRPSLK
	HSP60	Cell rescue, defense and virulence	Y495	LIDEpYGGDFAK
	HSP60	Cell rescue, defense and virulence	T377 or T379	GSIDIpTTPtNSYEK
	ILV2	Amino acid metabolism	S52	SASPLPAPSKRPEPAPSFNVDPLEQPAEPSK
	IRA1	Cellular communication / signal transduction	S497	IFpSLDDISSFNSSR
	MDS3	Unknown	S618	LSpSSGSLDNYFEK
	PDR5	Transport	S58	TLTAQSMQNpSTQSApNK
	PUP2	Protein fate	S56	ATpSPLESSEIEK
	SSC1	Protein fate	S61	IIENAEGpSR
	TDH1	Energy	T199	GGRpTASGNIIpSSTGAAK
	TIF4631	Protein synthesis	S908	DAPPASKDPpFITTR
	TOM70	Protein fate	T228 + (T230 or T232)	FGDIDpTApTApTPTTELSTQPAK
	TOM71	Protein fate	S76	QSEAFAGQNEDEADLKDDGpSVpSGSNKR
	TOM71	Protein fate	S96	AKpSGEGFDYpSLPNGEPDIAQLK
	YLH47	Unknown	S71	TTDGNQESASKVpSPVKEK
	ZRG8	Unknown	S403	VYSLNpSDEYSVNEK
	ZRG8	Unknown	S163	TTDSPLPAIK
	ZRG8	Unknown	S519	FEETpSLKSNK
ACH1	Lipid metabolism	S397	MLNGLGGpSADFLR	
Lactate + Galactose (16)	AC01	Amino acid metabolism	S298	pSMIEYLEATGR
	CAT2	Lipid metabolism	S514	SVpSTASLEFVSK
	CIT1	Energy	T239	IpTSTDPNADYgK
	CIT2	Energy	S14 or Y15	NVApSpYLQSNSSQEK
	COR1	Energy	T172	VLEHLHSTAFQNPtPLSLPTR
	COX4	Energy	T58	EGTVpPtDLDQETGLAR
	CYB2	Energy	T390	AMKKpTNVRRSOGA5R
	GUT2	Energy	T438	GSAPtQGVVR
	HER1	Unknown	S157	SSpSISTSLNER
	MCR1	Energy	S37	NQHpSFVFNESNK
	MDV1	Mitochondria biogenesis	S27 or S29 or T31	pSNpSNpTQDVLtNNGPYK
	PDH1	C-compound and carbohydrate metabolism	S250	KpSWAAGDAVSR
	PDH1	C-compound and carbohydrate metabolism	T51	YVHEpTPLK
	TOM70	Protein fate	S596	IRpSDPVLAK
	UIP4	Unknown	S185	ELpSPNFSEQETENKQDK
	Lactate + Glucose (2)	CYR1	Cellular communication / signal transduction	T389
SUR7		Unknown	S221	LASTYpSIDNSR
Lactate (4)	CAT2	Lipid metabolism	S25	MHpSAIVNYSTQK
	CIT2	Energy	S8	TVPYLNpSNR
	ICL2	C-compound and carbohydrate metabolism	T82 or s83 or S87 or S88	GSLPANpTpSIYpSpSYOAR
	SDH1	Energy	S449	LGANpSLLDLVVfGR

3.3. Variations of mitochondrial protein abundances and protein phosphorylation according to their metabolic pathways

Proteins whose amounts vary according to conditions were associated with the main metabolic pathways (Fig. 3, panel A) according to the MIPS functional classification (<http://mips.helmholtz-muenchen.de/genre/proj/yeast/>) and SGD

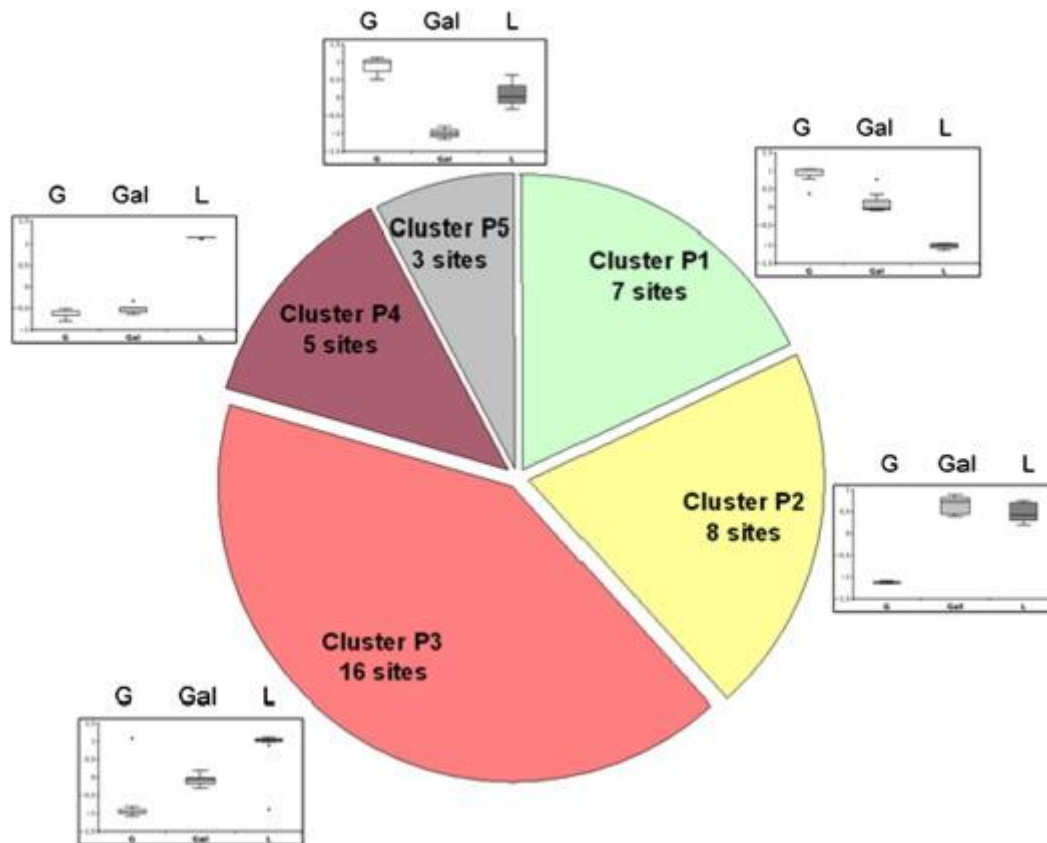


Fig. 2–Significant changes of phosphorylation level according to the substrate for the 39 varying residues quantified in the 3 growth conditions. Pie graph of the clusters built for phosphorylation sites whose abundance was significantly affected by the substrate (K-means clustering) (G = glucose; Gal = galactose; L = lactate). Box plots are depicted beside their respective shares. The number of phosphorylation sites associated to each of the five defined clusters is given.

(<http://www.yeastgenome.org/>) The pathways were affected differentially and two major patterns could be identified. Firstly, proteins involved in protein fate, amino acid metabolism, transport, C-compound and carbohydrate, vitamins and cofactors metabolism were mainly LAC-. Secondly, proteins involved in energy, protein synthesis and mitochondria biogenesis were

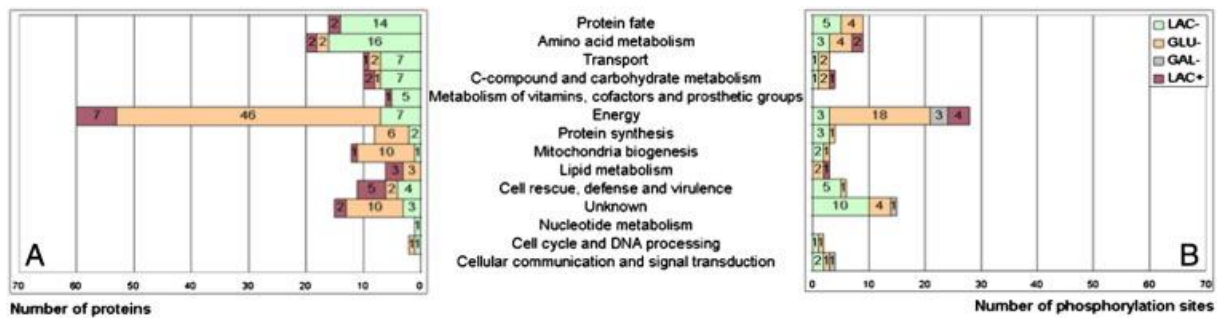


Fig. 3—Regulation of proteins abundance and protein phosphorylation status for different metabolic pathways. Distribution of varying proteins (A) and varying phosphorylation sites (B) in their 4 trends of regulation (LAC-, GLU-, LAC+, GAL-) for every metabolic pathway. For every metabolic pathway, the number of proteins and the number of phosphorylation sites associated to each trend are precised

mostly GLU-. For the other pathways (lipid metabolism, cell rescue, defense and virulence, nucleotide metabolism, cell cycle and DNA processing) the proteins did not appear to be grouped in any specific cluster, or the number of the proteins observed was too small to reach any significant conclusion. Accordingly, the metabolic pathway displaying the most variation of protein amount was energy metabolism that included enzymes of the respiratory chain and TCA cycle. They were all GLU-, i.e. more abundant in lactate and less in glucose, but differed by their abundance in galactose medium. It was of particular interest to note that the external NADH dehydrogenase Nde1p, the inhibitory peptide of the ATP synthase Inh1p and the TCA cycle enzyme Cit1p are accumulated in galactose medium, contrary to their respective functional homologs Nde2p, Stf1p and Cit3p (78%, 79% and 62% of homology, respectively). This suggests that growth in galactose medium might require the specific function of one specific homolog.

Phosphorylation sites whose status changed according to the carbon substrate were also associated with the metabolic pathway of the protein containing the residue (Fig. 3, panel B). Proteins of energy metabolism show the highest number of quantified sites displaying different phosphorylation levels. They were mainly dephosphorylated under glucose conditions. The other metabolic pathways did not show a general trend.

Our analysis gives deeper results on the mitochondrial changes at both proteomic and phosphoproteomic levels for every metabolic pathway. The most regulated metabolic pathway at both proteomic and phosphoproteomic levels was energy metabolism with 60 proteins exhibiting different abundances according to conditions and 28 phosphosites (20 phosphoproteins) showing different levels of phosphorylation as a function of growth medium. As the accumulation of the

respiratory complexes has been shown to be modified in fermentable conditions compared to a respirable one [1], we particularly focused our attention on the regulation of proteins involved in the respiratory chain. Interestingly, it must be noted that most of the protein chaperones involved in the assembly of the respiratory complexes were not regulated in the same way as the OXPHOS proteins, as no significant variation in their amount has been detected on the three different carbon sources (see Supplemental data S1).

3.4. Phosphorylation of proteins belonging to the oxidative phosphorylation display major variations between fermentative and respiratory growth and phosphorylation regulation is site-dependent

31 proteins involved in the respiratory chain were reproducibly quantified in the 3 growth conditions and showed different abundances according to the condition (Table 4). They are all GLU-, i.e. more abundant in lactate compared to glucose, which account for an increase in the oxidative phosphorylation during growth in respiratory conditions. 19 of these proteins were phosphorylated, displaying 37 phosphosites, which suggests an important role of phosphorylation in the regulation of the respiratory chain (Table 4). 12 of these residues located on 7 proteins exhibited a varying level of phosphorylation depending on the carbon source. For most of them, the level of phosphorylation globally varied in the same direction as protein amounts, as proteins were more abundant and more phosphorylated in respiratory conditions, except for 2 proteins. Rip1p was more abundant in lactate but more phosphorylated in glucose. Atp2p was also more abundant in lactate, but showed different phosphorylation patterns according to the residue: one residue was more phosphorylated in lactate (T43) but the two others (S35 and T40) were specifically less phosphorylated in galactose. Interestingly, 2 proteins (Cor1p and Atp2p) displayed several phosphorylation sites that were differentially regulated according to the substrate. Thus the variation of phosphorylation according to carbon substrate was site-dependent and not protein-dependent. Considering the position of the phosphosites on the complexes, most of the 37 quantified phosphosites are located on the matrix side, where the extra membrane parts of the complexes predominate while only one site, localized on Rip1p, is located in the intermembrane space (Fig. 4). When it was possible to look at the precise position in the structure, for Atp2p for example, we observed that the phosphorylation sites were at the periphery of the subunit which is in agreement with a good accessibility to kinases. Relations between kinases and their targets are still poorly documented in mitochondria: in particular for the mitochondrial proteins encoded by the nucleus, the question to know if phosphorylation occurs before or after their translocation to the mitochondria can be asked. However, some kinases have been shown to be located in the mitochondria (e.g. pyruvate dehydrogenase kinase [30] and protein kinase B, that phosphorylates Atp2p [31]) which seems rather in favor of a regulation within the organelle.

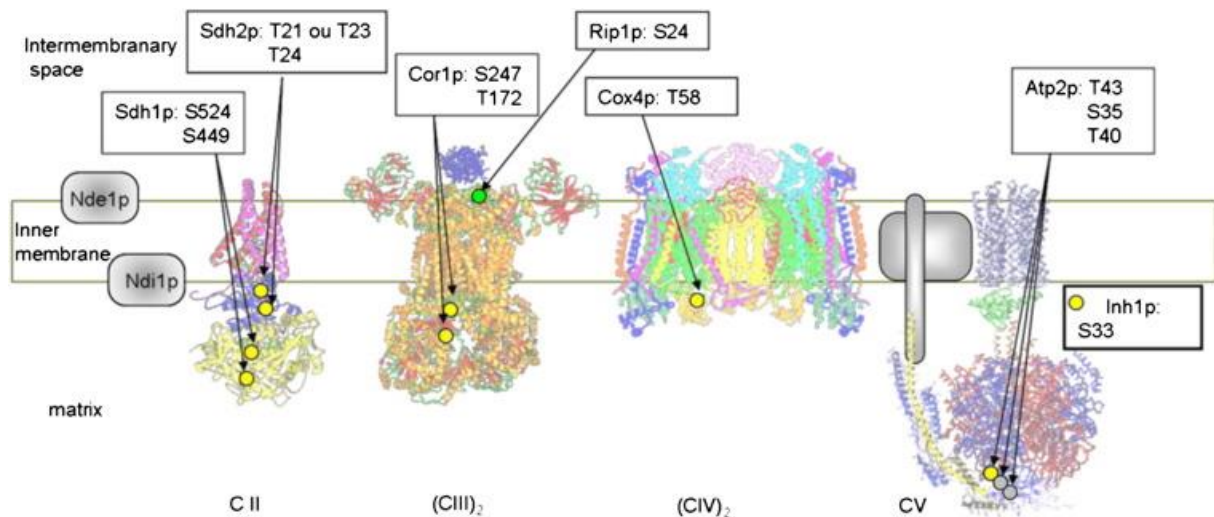


FIG. 4

Localization of phosphorylation sites on yeast OXPHOS proteins whose abundance vary according to conditions. The presented phosphoproteins exhibited different abundance according to growth conditions. Their phosphorylation sites also displayed either a consistent qualitative variation or a significant quantitative variation. Residues represented by a yellow point are those more phosphorylated in respiratory medium. The one in green has a higher level of phosphorylation in glucose medium. Those in gray are less phosphorylated in galactose, specifically. C II = succinate ubiquinone reductase. C III = ubiquinone cytochrome c reductase. C IV = cytochrome c oxidase. C V = ATP synthase. Respiratory complexes presented in their dimeric form are noticed by a subscript 2. Phosphorylation site of Inh1p is not localized in its structure since only bovine structure of Inh1p is available.

We have been able for the first time to quantitatively analyze variations of respiratory chain at proteomic and phosphoproteomic levels during a change in carbon source. Among the 37 phosphorylation sites discussed here, 34 have not been described yet (see Supplemental data S4). The comparison of these modifications suggests an important role for phosphorylation in the regulation of the respiratory complexes and this study is essential to target the phosphorylation sites which may be involved in this process. Some phosphorylation sites, located on Rip1p and Atp2p, are of particular interest since modifications of protein abundances and of phosphorylation levels are not on the same way and further experiments to elucidate the role of these residues are currently under investigation

4. Conclusions

We performed a combined approach of quantitative proteomic and phosphoproteomic analysis of mitochondria from yeast grown on three different carbon sources: glucose, galactose and lactate. We highlighted significant

differences of the proteome between the two fermentative substrates studied which suggest that galactose could be finally considered as a substrate displaying an intermediate metabolism between fermentation (glucose medium) and respiration (lactate medium). Proteins involved in a same metabolic pathway seem to exhibit a specific pattern of accumulation among the carbon source. The most regulated metabolic pathway at both proteomic and phosphoproteomic levels was energy metabolism and particularly the proteins involved in oxidative phosphorylation. They are all more abundant in lactate and less in glucose but some differs by their abundance in galactose. Their phosphorylation level also varies according to the carbon substrate mostly in the same way as the protein accumulation with a few exceptions. Our extensive study provides for the first time confident quantitative data on mitochondrial phosphosites responses to different carbon substrates. It is a step forward in the analysis of regulation of mitochondrial proteins by phosphorylation.

Acknowledgments

This work has received financial support and encouragements from Pr Marc Le Maire and particularly from Dr Bruno Robert. We are grateful to Dr Francis Haraux for helpful discussions since the beginning of the project and for the design of the yeast respiratory chain presented in Fig. 4. We thank Mehdi Lembrouk and Thierry Balliau for technical assistance and Aurélie Stanislas for the achievement of the preliminary experiments. We acknowledge Dr Patrice Hamel and Dr Andrew Gall for critical reading of the manuscript. We thank Pr Alexander Tzagoloff, Dr Manuel Garrigos and Dr Andy Pascal for their support. We thank Attila Csordas and the PRIDE team for their assistance in making the data available in the PRIDE repository. This work was supported by the International PhD Program for Life Science of CEA (IRTELIS) for which we sincerely thank Dr Christophe Carles.

Appendix A. Supplementary data

All the data on the protein and phosphopeptide identification are available on the following link: http://moulon.inra.fr/protic/yeast_mitochondria (login: mitochondria/password:review) The mass spectrometry proteomics data have been also deposited to the ProteomeXchange Consortium (<http://www.proteomexchange.org>) via the PRIDE partner repository [32] with the data identifiers PXD000714 and PXD000735 Projectname: Quantitative variations of the mitochondrial proteome and phosphoproteome during fermentative and respiratory growth in *Saccharomyces cerevisiae*. Supplementary data to this article can be found online at <http://dx.doi.org/10.1016/j.jprot.2014.04.022>.

REFERENCES

- [1] Schagger H, Pfeiffer K. Supercomplexes in the respiratory chains of yeast and mammalian mitochondria. *EMBO J* 2000;19:1777–83.
- [2] Acín-Pérez R, Fernández-Silva P, Peleato ML, Pérez-Martos A, Enriquez JA. Respiratory active mitochondrial supercomplexes. *Mol Cell* 2008;32:529–39.
- [3] Su B, Wang X, Zheng L, Perry G, Smith MA, Zhu X. Abnormal mitochondrial dynamics and neurodegenerative diseases. *Biochim Biophys Acta* 1802;2010:135–42.
- [4] Winklhofer KF, Haass C. Mitochondrial dysfunction in Parkinson's disease. *Biochim Biophys Acta* 2009;1802:29–44.
- [5] DiMauro S, Bonilla E, Davidson M, Hirano M, Schon EA. Mitochondria in neuromuscular disorders. *Biochim Biophys Acta* 1998;1366:199–210.
- [6] Maechler P, Wollheim CB. Mitochondrial function in normal and diabetic beta-cells. *Nature* 2001;414:807–12.
- [7] Verma M, Kagan J, Sidransky D, Srivastava S. Proteomic analysis of cancer-cell mitochondria. *Nat Rev Cancer* 2003;3:789–95.
- [8] Takahashi H, Iwai M, Takahashi Y, Minagawa J. Identification of the mobile light-harvesting complex II polypeptides for state transitions in *Chlamydomonas reinhardtii*. *Proc Natl Acad Sci U S A* 2006;103:477–82.
- [9] Bodenmiller B, Wanka S, Kraft C, Urban J, Campbell D, Pedrioli PG, et al. Phosphoproteomic analysis reveals interconnected system-wide responses to perturbations of kinases and phosphatases in yeast. *Sci Signal* 2010;3:rs4.
- [10] Schonberg A, Baginsky S. Signal integration by chloroplast phosphorylation networks: an update. *Front Plant Sci* 2012;3:256.
- [11] Oliveira AP, Ludwig C, Picotti P, Kogadeeva M, Aebersold R, Sauer U. Regulation of yeast central metabolism by enzyme phosphorylation. *Mol Syst Biol* 2012;8:623.
- [12] Griffin TJ, Gygi SP, Ideker T, Rist B, Eng J, Hood L, et al. Complementary profiling of gene expression at the transcriptome and proteome levels in *Saccharomyces cerevisiae*. *Mol Cell Proteomics* 2002;1:323–33.
- [13] Ohlmeier S, Kastaniotis AJ, Hiltunen JK, Bergmann U. The yeast mitochondrial proteome, a study of fermentative and respiratory growth. *J Biol Chem* 2004;279:3956–79.
- [14] Ohlmeier S, Hiltunen JK, Bergmann U. Protein phosphorylation in mitochondria. A study on fermentative and respiratory growth of *Saccharomyces cerevisiae*. *Electrophoresis* 2010;31:2869–81.
- [15] Pflieger D, Le Caer JP, Lemaire C, Bernard BA, Dujardin G, Rossier J. Systematic identification of mitochondrial proteins by LC–MS/MS. *Anal Chem* 2002;74:2400–6.
- [16] Sickmann A, Reinders J, Wagner Y, Joppich C, Zahedi R, Meyer HE, et al. The proteome of *Saccharomyces cerevisiae* mitochondria. *Proc Natl Acad Sci U S A* 2003;100:13207–12.

- [17]Reinders J, Zahedi RP, Pfanner N, Meisinger C, Sickmann A. Toward the complete yeast mitochondrial proteome: multidimensional separation techniques for mitochondrial proteomics. *J Proteome Res* 2006;5:1543–54.
- [18]Boersema PJ, Raijmakers R, Lemeer S, Mohammed S, Heck AJ. Multiplex peptide stable isotope dimethyl labeling for quantitative proteomics. *Nat Protoc* 2009;4:484–94.
- [19]Lemaire C, Dujardin G. Preparation of respiratory chain complexes from *Saccharomyces cerevisiae* wild-type and mutant mitochondria: activity measurement and subunit composition analysis. *Methods Mol Biol* 2008;432:65–81.
- [20]Meisinger C, Sommer T, Pfanner N. Purification of *Saccharomyces cerevisiae* mitochondria devoid of microsomal and cytosolic contaminations. *Anal Biochem* 2000;287:339–42.
- [21]Reinders J, Wagner K, Zahedi RP, Stojanovski D, Eyrich B, vander Laan M, et al. Profiling phosphoproteins of yeast mitochondria reveals a role of phosphorylation in assembly of the ATP synthase. *Mol Cell Proteomics* 2007;6:1896–906.
- [22]Bonhomme L, Valot B, Tardieu F, Zivy M. Phosphoproteome dynamics upon changes in plant water status reveal early events associated with rapid growth adjustment in maize leaves. *Mol Cell Proteomics* 2012;11:957–72.
- [23]Valot B, Langella O, Nano E, Zivy M. MassChroQ: a versatile tool for mass spectrometry quantification. *Proteomics* 2011;11:3572–7.
- [24]Benjamini Y, Hochberg Y. Controlling the false discovery rate: a practical and powerful approach to multiple testing. *J Roy Stat Soc B* 1995;57:289–300.
- [25]Margeot A, Garcia M, Wang W, Tetaud E, di Rago JP, Jacq C. Why are many mRNAs translated to the vicinity of mitochondria: a role in protein complex assembly? *Gene Cross-Talk between Nucleus and Organelles*, 354; 2005 64–71.
- [26]Futcher B, Latter GI, Monardo P, McLaughlin CS, Garrels JI. A sampling of the yeast proteome. *Mol Cell Biol* 1999;19:7357–68.
- [27]Prokisch H, Scharfe C, Camp II DG, Xiao W, David L, Andreoli C, et al. Integrative analysis of the mitochondrial proteome in yeast. *PLoS Biol* 2004;2:e160.
- [28]Lagunas R. Misconceptions about the energy metabolism of *Saccharomyces cerevisiae*. *Yeast* 1986;2:221–8.
- [29]Amoutzias GD, He Y, Lilley KS, Van de Peer Y, Oliver SG. Evaluation and properties of the budding yeast phosphoproteome. *Mol Cell Proteomics* 2012;11:1–13.
- [30]Muller G, Bandlow W. Protein phosphorylation in yeast mitochondria: cAMP-dependence, submitochondrial localization and substrates of mitochondrial protein kinases. *Yeast* 1987;3:161–74.
- [31]Bijur GN, Jope RS. Rapid accumulation of Akt in mitochondria following phosphatidylinositol 3-kinase activation. *J Neurochem* 2003;87:1427–35.

[32]Vizcaino JA, Cote RG, Csordas A, Dianas JA, Fabregat A, FosterJM, et al. The PRoteomics IDentifications (PRIDE) database and associated tools: status in. *Nucleic Acids Res* 2013;41:D1063–9.

Table 4–Phosphorylation of OXPHOS proteins whose abundance change according to growth conditions. Phosphorylation sites displaying a significant quantitative variation were noted in bold with 1 asterisk and those displaying a consistent qualitative variation were noted in bold with 2. Positions of the phosphorylated amino acids were determined from precursor proteins. Phosphorylation sites unambiguously located on the peptide sequence are indicated in bold and by p in the sequence. Otherwise, the different possibilities are noted in the sequence.

ORF	Gene	Phosphorylation site	Group of regulation for level of phosphorylation	Phosphopeptide
YML120C YMR145	NDI1	S27		pSpTGVENSGAGPTSFK

CNDE1S265AASLpSPKDPERYDL085WNDE2YKL148CSDH1S524*GLU–TQpSpSLDE
 GVRS449**GLU–LGANpSLLDLWFGRYLL041CSDH2T21ouT23*GLU–ApTApTTAA
 ATHTPRT24**GLU–ATATpTAAATHTPRYKL141WSDH3T30 ou
 T28ATATTAAPpTHpTPRYDR178WSDH4YOR065WCYT1YEL024WRIP1S24*GLU+Ip
 SQpSLLASKYBL045CCOR1S247*GLU–AAFLGpSEVRT172**GLU–VLEHLHSTAFQN
 pTPLpSLPTRS94 ou S95 ou
 S98EGLALpSpSNIpSRS135ANLLSpSpSNFEATKT24LATAVApTPKYPR191WQCR2S33
 4NAVQNESVSpSPIELNFDKDFKYDR529CQCR7YJL166WQCR8YHR001W-
 AQCR10S5AYTpSHLSSKS8AYTSHLpSSKQ0250COX2YGL187CCOX4T58**GLU–EGT
 VPpTDLQETGLARYNL052WCOX5AS92RPVLNKGDPpSSFIKKS93GDSpSFIKYG
 L191WCOX6A = COX13YLR038CCOX6B =
 COX12S7ADQENpSPLHTVGFDAARYLR395CCOX8YBL099WATP1S178RpSVHEPVQT
 GLKT38 ou S37ApSpTKAQPTEVSSI
 LEERS57IKGVpSDEANLNETGRT43AQPpTEVSSILEERS47AQPTEVSpSILEERYJR121
 WATP2T40*GAL–ASAAQSpTPITGKT43*GLU–ASAAQSTPIpTGKS35*GAL–ApSAAQ
 STPITGKS39ASAAQpSTPITGKS299FTQAGpSEVSALLGRYBR039WATP3S226TIEQSP
 pSFG

KFEIDTDANVPRYDR298CATP5S48NpSSIDAAFQSLQKYLR295CATP14T92AYTEQN
VEpTAHVAKYDL004WATP16S29 ou
S30AEAAAAPSpSGLKYDR377WATP17S23NIGpSAPNAKYML081C-
AATP18YPR020WATP20YDR322C-AATP21 =
TIM11INH1S33GLU-GpSGSEDSFVKRS38GSGSEDpSFVKR148
JOURNAL OF
PROTEOMICS 106 (2014) 140–150